

FrogDogNet: Fourier frequency Retained visual prompt Output Guidance for Domain Generalization of CLIP in Remote Sensing

Hariseetharam Gunduboina¹

Muhammad Haris Khan²

Biaplal Banerjee¹

¹Indian Institute of Technology Bombay, India

²Mohamed Bin Zayed University of Artificial Intelligence, UAE

hariseetharam552@gmail.com, muhammad.haris@mbzuai.ac.ae, getbiaplal@gmail.com

Abstract

In recent years, large-scale vision-language models (VLMs) like CLIP have gained attention for their zero-shot inference using instructional text prompts. While these models excel in general computer vision, their potential for domain generalization in remote sensing (RS) remains under-explored. Existing approaches enhance prompt learning by generating visual prompt tokens but rely on full-image features, introducing noise and background artifacts that vary within a class, causing misclassification. To address this, we propose *FrogDogNet*, a novel prompt learning framework integrating Fourier frequency filtering and self-attention to improve RS scene classification and domain generalization. *FrogDogNet* selectively retains invariant low-frequency components while eliminating noise and irrelevant backgrounds, ensuring robust feature representation across domains. The model first extracts significant features via projection and self-attention, then applies frequency-based filtering to preserve essential structural information for prompt learning. Extensive experiments on four RS datasets and three domain generalization tasks show that *FrogDogNet* consistently outperforms state-of-the-art prompt learning methods, demonstrating superior adaptability across domain shifts. Our findings highlight the effectiveness of frequency-based invariant feature retention in generalization, paving the way for broader applications. Our code is available at <https://github.com/HariseetharamG/FrogDogNet>

1. Introduction

Remote Sensing (RS) image analysis underpins a diverse range of tasks including Earth observation [18], environmental monitoring [35, 90], urban planning [62], and disaster management [39, 104], to name a few. Although deep learning models have substantially advanced RS analytics [69], they often exhibit performance drops under domain

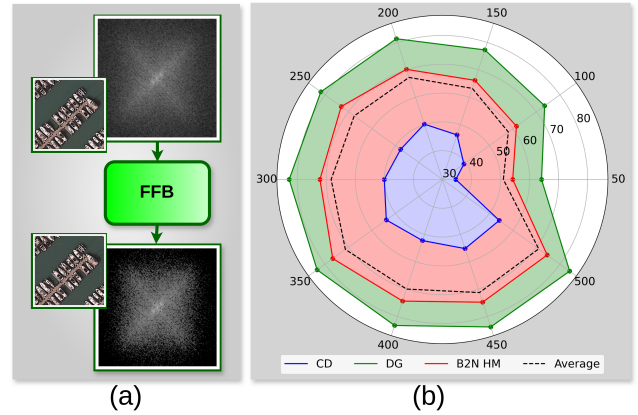


Figure 1. Impact of Fourier Filtering on RS Image Analysis: (a) demonstrates that retaining 50% of low-frequency components (LFCs) preserves structural details while reducing noise in the frequency magnitude spectrum. (b) presents a sensitivity analysis, showing that keeping 350 out of 512 LFCs of visual features $f_v(x)$ achieves the highest average generalization performance.

shifts—variations in sensor modalities, atmospheric conditions, and geographical characteristics that cause discrepancies between training (source) and testing (target) data distributions. Two core strategies address such shifts: domain adaptation (DA), which aligns source and target distributions during training [26, 29, 91, 100], and domain generalization (DG), which strives for robust performance in unseen target domains [25, 48, 133, 137]. DG is crucial in RS due to the difficulty of collecting labeled target-domain data. Challenges include cross-sensor variability, seasonal and atmospheric changes, geographic distribution shifts, and limited real-time data for disaster monitoring [36, 72, 100, 142]. Despite progress via adversarial training [70], meta-learning [116], and domain-invariant representations [32, 117], existing DG approaches struggle to handle the extreme spectral and spatial variations in RS datasets. Beyond domain shifts, RS tasks typically suffer from limited annotated data, as labeling requires domain expertise (e.g., differentiating land-use categories or vegetation types). The substantial cost and logistical complexity of labeling across

diverse environments hamper large-scale data curation, exacerbating the challenge of building robust models. Few-shot learning (FSL) [13, 28, 41, 89, 124] partially addresses this issue by enabling models to learn from minimal supervision. Although FSL has been explored for multispectral and hyperspectral RS imagery [2, 64, 73, 115], most methods remain image-centric, inadvertently capturing extensive background clutter in RS scenes, such as oceans, deserts, or forests. Since key objects of interest (e.g., urban structures, agricultural plots) are often small and spatially scattered, Standard FSL pipelines optimized for natural images often generalize poorly when applied to RS datasets. This is validated in our work, where methods like CLIP [81], CoOp [139] and CoCoOp [138] struggle with RS data.

Vision-Language Models (VLMs) like CLIP [81], ALIGN [43], Florence [118], and LiT [123] leverage textual supervision for powerful zero-shot adaptation. Adaptations for RS (e.g., RS-CLIP [56], RemoteCLIP [65], and ChangeCLIP [21]) illustrate the promise of combining visual and textual cues but remain challenged by large homogeneous backgrounds and small, high-value objects in RS. Although prompt-learning techniques [7, 31, 45, 138–140] have been proposed to refine VLMs for downstream tasks, most still operate on entire images, rendering them susceptible to overfitting on dominant yet irrelevant features. Multi-scale methods [6, 95] address some of these challenges but often lack a robust mechanism to filter out noise and irrelevant background artifacts. This limitation reduces their effectiveness, particularly under varying spectral conditions where such artifacts can significantly degrade performance.

To address these gaps, we propose leveraging Fourier Transform-based filtering to enhance DG for RS image analysis. Fourier filtering is widely employed in RS for denoising and spectral feature extraction, as it separates low-frequency semantic structures from high-frequency noise and sensor artifacts. This property reduces sensitivity to environmental variations and promotes stable feature extraction. However, filtering out high-frequency components too aggressively can discard fine-grained details critical for object boundaries. To mitigate this, we introduce a self-attention mechanism [106] that selectively retains local cues while preserving robustness under domain shifts. As illustrated in Figure 1(a), retaining the top 50% low-frequency components (LFC) effectively removes high-frequency clutter but can risk losing valuable details. Our analysis in Figure 1(b) indicates that retaining 350 out of 512 LFCs yields the best average performance across multiple RS datasets and generalization tasks.

We introduce a **FrogDogNet** (*Fourier frequency Retained visual prompt Output Guidance for Domain Generalization of CLIP in Remote Sensing*) framework for few-shot RS recognition, integrating a Fourier Filter Block (FFB) within a CLIP-based pipeline. The FFB focuses

on semantically relevant structures while discarding background clutter, thereby improving domain generalization. A Prompt Alignment Loss aligns learned prompts with RS-specific initializations, bolstering transferability across diverse imaging conditions. To further refine feature representations, we design a lightweight Meta-Net that converts filtered embeddings into tokens optimized for downstream tasks. Our principal contributions are threefold:

- **Fourier Filter Block (FFB):** We propose a dedicated block that isolates essential low-frequency RS features, suppresses noise, and, combined with self-attention, selectively preserves crucial object boundaries.
- **Remote Sensing Prompt Alignment Loss:** We introduce a novel loss function that harmonizes learned prompts with various RS-specific text initializations, significantly enhancing zero-shot and few-shot adaptability.
- **Comprehensive Evaluation:** Extensive experiments on multiple RS benchmarks—including base-to-new class generalization, cross-dataset transfer, and multi-target adaptation—demonstrate the superior performance and practical value of our approach compared to existing methods.

2. Related Works

(a) Domain Generalization: Deep learning models often struggle with domain shifts, where discrepancies between training and testing distributions lead to performance degradation. DG aims to develop models that generalize to unseen domains without requiring target data. DG approaches can be categorized into multi-source DG (Multi-DG) and single-source DG (Single-DG). Multi-DG methods leverage meta-learning [27, 48], regularization techniques [4, 24, 59], adversarial training [51, 58, 71], and domain augmentation [113, 135, 136]. Other strategies include gradient-based dropout [38], episodic training [49], and domain-specific masking [11].

Single-DG, a more challenging yet practical setting, trains models on a single domain while ensuring generalization to unseen domains. Solutions include domain expansion [53, 77, 78, 108, 112, 114], adversarial attacks [78, 98, 108, 131], information bottleneck [99], contrastive learning [53], and uncertainty estimation [77]. Despite substantial progress in standard vision tasks, DG for RS image classification remains underexplored [74, 133]. Given the high spectral variability, heterogeneous textures, and geographically induced domain shifts in RS data, further research is needed to achieve improved generalization.

(b) Vision-Language Models in RS: Foundation models, particularly large-scale Vision-Language Models (VLMs) [42, 82, 118], have significantly advanced computer vision by learning robust multimodal representations. Models like CLIP [81] and VisualBERT [54] have outperformed traditional vision models across various tasks but face challenges in unimodal learning for complex applications such

as image captioning [107] and visual question answering [3]. VLMs achieve generalization by combining pre-trained textual embeddings (e.g., BERT [20], GPT [80]) with visual representations from CNNs or Vision Transformers [22].

With the increasing availability of textual metadata, VLMs are being actively explored for RS applications [57, 101], including image captioning [55, 60, 67, 92, 111, 127, 128, 132, 143], text-based image retrieval [1, 16, 83, 85, 86, 119, 121, 122], and visual question answering [5, 10, 66, 84, 120, 134]. Other applications include scene classification [47, 61, 79, 97, 109], semantic segmentation [14, 129], and object detection [44, 68, 125].

Recent works have sought to optimize VLMs for RS by creating large-scale caption datasets. RS5M [130] introduced an automated caption dataset using BLIP-2 [52], while RS-GPT [37] developed human-annotated RSICap, integrating GPT-based models for captioning and visual question answering. As RS datasets continue to grow, VLMs are expected to become increasingly central to RS applications, but their adaptation to the unique spectral, spatial, and textual challenges of RS data remains an open problem.

(c) Prompt Learning for RS: Prompt learning, initially developed in natural language processing (NLP) [75], has gained traction in vision tasks by leveraging pre-trained language models for enhanced generalization. Automated prompt generation techniques, such as AutoPrompt [93], optimize prompts by identifying tokens that maximize gradient-based label likelihood. In the vision domain, CoOp [139] fine-tunes CLIP through learnable prompts for few-shot classification, while CoCoOp [138] extends this by conditioning prompts on image features to improve generalization. Similarly, CLIP-Adapter [31] fine-tunes lightweight adapters for visual and textual embeddings, and ProGrad [140] refines prompt tuning by preserving foundational knowledge. Other works, such as TPT [94], introduce predictive consistency across different views of the same image, while MaPLe [45] leverages coupled vision and language prompts for progressive learning, thereby enhancing robustness in a variety of recognition tasks.

In RS, prompt learning has been explored for scene classification [46, 63], few-shot learning [8, 9, 95], and segmentation [12, 110, 126]. To address complex textures and domain shifts in RS imagery, models like APLeNet [95], StyLIP [7], C-SAW [6], and RS3Lip [40] utilize multi-scale visual features, style-based prompts, or spatially-aware prompting.

3. Methodology

We introduce a novel visual prompt learning method (FrogDogNet) guided by Fourier filters to enhance domain generalization in the CLIP model for remote sensing. A detailed overview of FrogDogNet approach is presented in Figure 2. To provide context for FrogDogNet’s main architecture, we

begin by discussing relevant baseline models, such as CLIP [81], CoOp [139], and CoCoOp [138].

3.1. Preliminaries

CLIP [81] is a vision-language model that aligns visual and textual representations via contrastive learning. It comprises a visual encoder f_v (e.g., ResNet [34] or ViT [23]) for input images x and a text encoder f_t (BERT-based [19]) for text prompts of the form "a photo of $[CLS]_y$ ", where $[CLS]_y$ denotes class y . Given a batch of N image-caption pairs $B = \{(x_n, t_n)\}_{n=1}^N$, CLIP maximizes cosine similarity for the correct N pairs while minimizing it for the remaining $N^2 - N$ mismatched pairs. This is achieved through a symmetric multi-class contrastive loss [96]:

$$L_{\text{CLIP}} = -\frac{1}{N} \sum_{n=1}^N \left[\log p(t_n | x_n) + \log p(x_n | t_n) \right], \quad (1)$$

where

$$p(t_n | x_n) = \frac{\exp(\text{sim}(f_v(x_n), f_t(t_n))/\tau)}{\sum_{m=1}^N \exp(\text{sim}(f_v(x_n), f_t(t_m))/\tau)}, \quad (2)$$

$$p(x_n | t_n) = \frac{\exp(\text{sim}(f_t(t_n), f_v(x_n))/\tau)}{\sum_{m=1}^N \exp(\text{sim}(f_t(t_n), f_v(x_m))/\tau)}, \quad (3)$$

$\text{sim}(\cdot, \cdot)$ denotes cosine similarity and τ is the temperature parameter. By training on a large-scale dataset of 400 million image-text pairs, CLIP effectively aligns images with textual descriptions for zero-shot transfer.

Despite its robustness, CLIP relies on manually crafted prompts, limiting flexibility across domains. **CoOp** [139] addresses this by introducing learnable prompts—context vectors optimized via backpropagation in place of static templates, structured as $t_y = \{[c_1], [c_2], \dots, [c_M], [CLS_y]\}$, where t_y represents the prompt for class y , $[c_1] \dots [c_M]$ are the M learnable context tokens. However, CoOp often struggles with domain shifts.

CoCoOp [138] improves generalization by conditioning prompt learning on visual features through a meta-network that refines context vectors dynamically, thereby allowing adaptation across diverse inputs. Yet, CoCoOp remains less effective in specialized fields like remote sensing and medical imaging, where unique image characteristics demand more tailored fine-tuning strategies.

Motivation: In RS, crucial class-defining features are frequently entangled with irrelevant backgrounds, leading to non-stationary semantics. Our FrogDogNet approach selectively propagates only the most discriminative, consistent features for each class, filtering out irrelevant information to focus on class-representative content. This targeted strategy, validated in Figure 1, enhances robustness and classification accuracy. In contrast, CoCoOp employs all image features indiscriminately, resulting in less effective domain transfer for RS tasks.

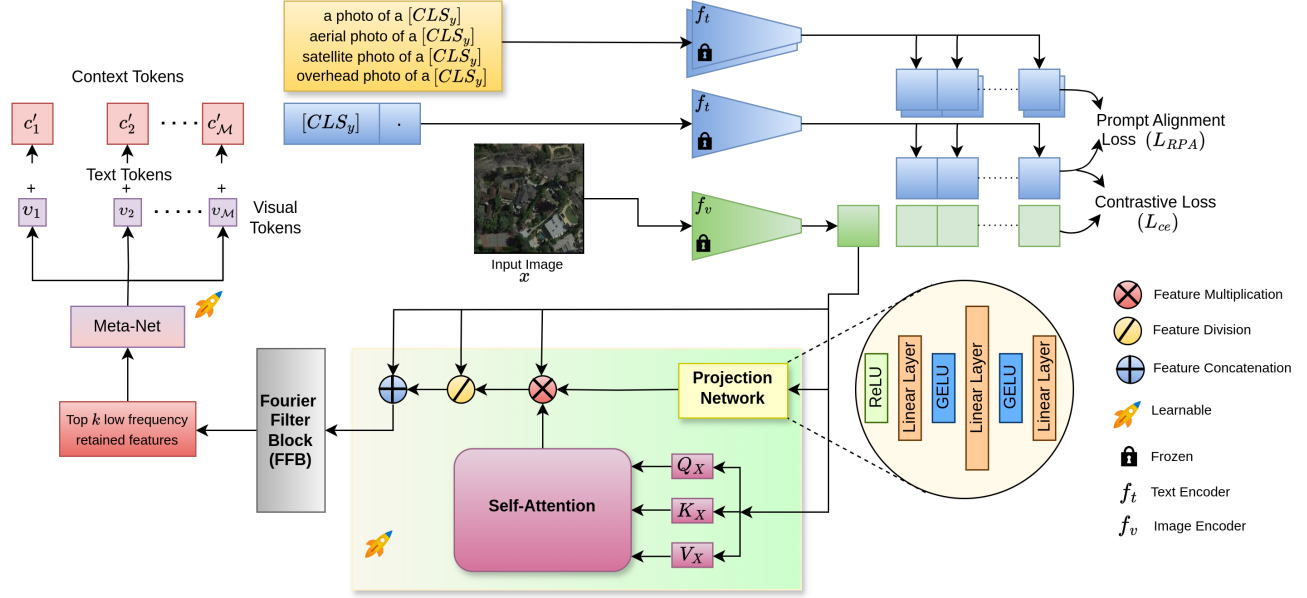


Figure 2. Overview of FrogDogNet comprises a text encoder (f_t), an image encoder (f_v), a projection network, self-attention, and a Fourier Filter Block (FFB) for refining visual features. The image encoder extracts features, which are processed through the projection network and self-attention with residual connections, while the FFB retains key low-frequency components. The refined features pass through a lightweight Meta-Net $\{h_m\}_{m=1}^M$ to generate visual tokens $\{v_m\}_{m=1}^M$, which are combined with learnable text tokens $\{c_m\}_{m=1}^M$ and class embeddings before entering the text encoder. To align the learned text prompts with remote sensing (RS) prompts, we introduce RS Prompt Alignment (RPA) loss. The model is trained using a multi-task objective, incorporating both contrastive loss and RPA loss.

To propagate only the most discriminative features into FrogDogNet’s prompt learning pipeline, we leverage the **Discrete Fourier Transform (DFT)** and its computationally efficient variant, the Fast Fourier Transform (FFT) [17], reduce the complexity from $O(P^2)$ to $O(P \log P)$ [87]. For a discrete sequence $\{s_p\}$ of length P , with $p \in [0, P - 1]$, the one-dimensional (1D) DFT is defined as:

$$S_q = \sum_{p=0}^{P-1} s_p e^{-i \frac{2\pi}{P} pq}, \quad 0 \leq q \leq P - 1. \quad (4)$$

In two-dimensional settings (e.g., images), the 1D DFT is applied along both rows and columns, forming the 2D DFT:

$$S_{(q,r)} = \sum_{p=0}^{P-1} \sum_{t=0}^{T-1} s_{(p,t)} e^{-i \frac{2\pi}{P} pq} e^{-i \frac{2\pi}{T} tr}, \quad (5)$$

where $s_{(p,t)}$ represents the spatial domain input, $S_{(q,r)}$ is the transformed representation, and P, T denote the respective dimensions. By transforming images or feature embeddings into the frequency domain, we can retain only a fraction of LFC—those capturing the dominant spatial structures—while discarding high-frequency details often associated with noise or irrelevant content. The Inverse FFT (IFFT) then reconstructs the filtered images or embeddings back into the spatial domain. This approach introduces a novel advancement in visual prompt learning, addressing a limitation in earlier methods where all image features, including noise, were used in the optimization process, leading to suboptimal performance. In contrast, this method re-

tains only the most significant visual features for prompt tuning, which are also redundant within the class, enabling the model to outperform all major prompting baselines.

3.2. Model architecture of FrogDogNet

Now coming to the main model, as shown in the Figure 2, we passed the image feature embeddings $f_v(x)$ to the Projection Network and Self Attention sections with residual connections, before passing to the FFB.

3.2.1. Projection Network

Let us consider $f_v(x) = X$, representing the image embeddings. Our goal is to refine these embeddings while preserving key information. Let $X \in \mathbb{R}^{B \times d}$ be the input to the projection network, where B is the batch size and d is the feature dimension. We first apply a linear transformation:

$$X' = W_1 X + b_1, \quad (6)$$

using learnable weights $W_1 \in \mathbb{R}^{d \times d}$, where X' represents the transformed feature embeddings. A Gaussian Error Linear Unit (GELU) activation introduces smooth non-linearity, followed by an expansion step:

$$X'' = W_2 \text{GELU}(X') + b_2, \quad (7)$$

where X'' increases the feature dimension from d to $2d$ via $W_2 \in \mathbb{R}^{d \times 2d}$. After another GELU activation, the features are projected back to d dimensions, denoted as X''' :

$$X''' = W_3 \text{GELU}(X'') + b_3, \quad (8)$$

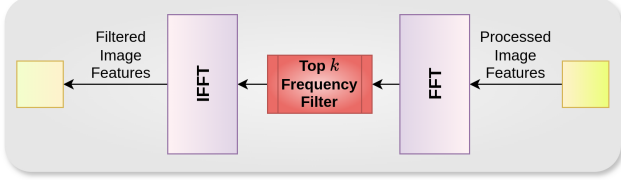


Figure 3. The Fourier Filter Block (FFB) transforms image embeddings X using Fast Fourier Transform (FFT), retains the top k frequencies, and applies Inverse FFT (IFFT) to map them back to the original embedding space.

where $W_3 \in \mathbb{R}^{2d \times d}$, and b_1, b_2, b_3 are bias terms. Finally, a ReLU activation is applied to encourage sparse activations, and its output is multiplied by X to form a residual connection. Let the final output be $X_{\text{projector}}$:

$$X_{\text{projector}} = \text{ReLU}(X''') \cdot X. \quad (9)$$

3.2.2. Proposed Self-Attention Module

To capture complex dependencies among visual features X , we introduce a self-attention mechanism where the same input features serve as the query, key, and value:

$$\text{Attention}(Q = X, K = X, V = X). \quad (10)$$

Specifically, each feature vector attends to all others using scaled dot-product attention:

$$X_{\text{self}} = \text{Attention}(Q, K, V) = \text{Softmax}\left(\frac{QK^T}{\sqrt{d}}\right)V, \quad (11)$$

where d denotes the feature dimension. These attention scores modulate the contribution of each value vector to the final output, enabling the model to dynamically aggregate contextual information. Additionally, we scale the outputs from the Projection Network ($X_{\text{projector}}$) and the self-attention module (X_{self}) by a tunable factor λ to regulate their influence within the architecture:

$$X_{\text{out}} = \lambda \cdot X_{\text{projector}} \cdot X_{\text{self}}, \quad (12)$$

and subsequently normalize X_{out} by dividing it by X . We then incorporate a residual connection by adding X :

$$X_{\text{final}} = X_{\text{out}}/X + X. \quad (13)$$

We refer to X_{final} as the *Processed Image Features* (PIFs), which are passed to the FFB for further refinement.

3.2.3. Fourier Filter Block (FFB)

We pass the PIFs to the FFB, where they are transformed from the spatial domain to the frequency domain using FFT. We then retain top k LFC, which capture the most salient yet class-redundant information in the embeddings, and apply an inverse IFFT to map the filtered features back to the spatial domain. Figure 3 provides an overview of this process.

After filtering, the resulting retained features $\psi \in \mathbb{R}^{B \times d}$ are fed into a lightweight neural network, termed the *Meta-Net*, following the design in [138]. The Meta-Net consists

of a set of learnable functions $\{h_m\}_{m=1}^{\mathcal{M}}$ that generate \mathcal{M} visual tokens $\{v_1, \dots, v_{\mathcal{M}}\}$ according to:

$$v_m = h_m(\psi). \quad (14)$$

Each visual token v_m is then added to its corresponding textual token c_m to form the m^{th} prompt token:

$$c'_m = c_m + v_m. \quad (15)$$

Collectively, these tokens compose the prompt:

$$t_y = \{[v_1 + c_1], \dots, [v_{\mathcal{M}} + c_{\mathcal{M}}], [CLS_y]\}. \quad (16)$$

By leveraging the most informative frequency components through the FFB and integrating them with textual embeddings via Meta-Net, this approach enhances prompt generation and yields stronger contextual representations.

3.3. Loss functions, training, and inference

We adopt a multi-task learning strategy with two complementary loss functions. First, we employ a *supervised contrastive loss* \mathbf{L}_{ce} to promote alignment between the visual feature representation $f_v(x)$ and the textual feature representation $f_t(t_y)$. This loss is realized via cross-entropy, ensuring accurate classification of seen classes.

To further enhance adaptability under various RS prompt initializations, we introduce a *Remote Sensing Prompt Alignment Loss* \mathbf{L}_{RPA} , motivated by [33]. Formally, the label prediction for an input x is given by

$$p(y | x) = \frac{\exp(\text{sim}(f_v(x), f_t(t_y(\psi_\phi(x))))/\tau)}{\sum_{k=1}^{|\mathcal{Y}|} \exp(\text{sim}(f_v(x), f_t(t_k(\psi_\phi(x))))/\tau)}, \quad (17)$$

where ϕ indicate the learnable parameters upto FFB.

Let $\mathcal{D}_s = \{\mathcal{D}_s^i\}_{i=1}^n$ be n source domains with inputs $x^i \in \mathcal{X}^i$ and labels $y^i \in \mathcal{Y}_{\text{Seen}}$, where $P(\mathcal{D}_s^i)$ varies. Training uses $\mathcal{Y}_{\text{Seen}}$, while testing is on a target domain \mathcal{D}_t with unseen labels $\mathcal{Y}_{\text{Unseen}}$ and $P(\mathcal{D}_t) \neq P(\mathcal{D}_s^i)$.

The cross-entropy loss \mathbf{L}_{ce} is defined as

$$\mathbf{L}_{\text{ce}} = \arg \min_{\psi_\phi, \{h_m\}} \mathbb{E}_{(x,y) \in \mathcal{P}(\mathcal{D}_s)} \left[- \sum_{k=1}^{\mathcal{Y}_{\text{Seen}}} y_k \log(p(y_k | x)) \right]. \quad (18)$$

We denote the textual embeddings from CLIP and from our model as $c_i^{\text{clip}} = f_t(t_i^{\text{clip}})$ and $c_i = f_t(t_i)$, respectively. Minimizing the Euclidean distance between c_i and c_i^{clip} strengthens alignment with RS-specific prompts, thereby improving generalization on unseen classes. Hence, we define the *Remote Sensing Prompt Alignment Loss*:

$$\mathbf{L}_{\text{RPA}} = \frac{1}{Z} \sum_{z=1}^Z \left(\frac{1}{N_c} \sum_{i=1}^{N_c} \|c_i - c_{z_i}^{\text{clip}}\|^2 \right), \quad (19)$$

where $\|\cdot\|_2$ denotes the Euclidean norm, N_c is the number of seen classes, and Z is the total number of RS prompt variants. During inference, the model leverages

these aligned prompts to enhance classification accuracy on unseen classes. Finally, the *total loss* function is:

$$\mathbf{L}_{\text{total}} = \arg \min_{\psi_{\phi}, \{h_m\}} [\mathbf{L}_{\text{ce}} + \Lambda \cdot \mathbf{L}_{\text{RPA}}], \quad (20)$$

where Λ is a hyper-parameter that balances the contributions of \mathbf{L}_{ce} and \mathbf{L}_{RPA} . During inference, cosine similarity is calculated between the image $x_t \in \mathcal{D}_t$ and the prompt embeddings of all classes in $\mathcal{Y}_{\text{Unseen}}$. The class with the highest similarity score is assigned as the predicted label:

$$\hat{y}_t = \arg \max_{y \in \mathcal{Y}_{\text{Unseen}}} p(y|x_t). \quad (21)$$

4. Experimental Evaluations

Datasets: We experiment on four RS datasets: **PatternNet** [50] (38 classes, 800 images/class, 256×256), **RSICD** [67] (30 classes, 10,000 images, 224×224), **RESISC45** [15] (45 classes, 700 images/class, 256×256), and **MLRSNet** [76] (46 classes, 109,161 images, 256×256). Following [95], we use their **v2** version with 16 overlapping classes. Further details are in the supplementary material.

Architecture: As described in Section 3.2, we use a projection network followed by a self-attention block with 4 attention heads. The resulting PIFs pass through the FFB, where we experiment with retaining various numbers of top k low-frequency features. We fix $k = 350$ out of 512 image features (based on Figure 1(b), detailed explanation is presented in supplementary material) and project these filtered image features ψ into the light weight Meta-Net to match the dimensionality of the text embeddings.

Training and evaluation: We train for 50 epochs using SGD [88] with an initial learning rate of 2×10^{-3} and a warm-up rate of 1×10^{-5} for the first epoch. Following Figure 8, we use ViT-B/16 as the image encoder and train with 16 shots per class, a batch size of 4, and prompt variants $Z = 4$ (shown in Figure 2). Based on extensive experiments, we set $\lambda = 0.3$ in Equation 12 and we set $\Lambda = 0.5$ in Equation 20, analysis shown in Figure 7. Text prompts follow the template "a photo of a [CLS]" with a context length of four, consistent with prior works [138, 139]. We report top-1 average accuracy over three random seeds.

4.1. Comparison to the literature

We compare the performance of FrogDogNet with existing state-of-the-art (SOTA) methods (explained in supplementary) for three domain generalization tasks like [95].

1. Base-to-New Class Generalization (B2N): Evaluates the model’s ability to generalize to classes not seen during training, ensuring $\mathcal{Y}_{\text{Seen}} \cap \mathcal{Y}_{\text{Unseen}} = \emptyset$. **2. Cross-Dataset Generalization (CD):** Involves training on one dataset and testing on other datasets with different domain distributions and label sets, ensuring $\mathcal{Y}_{\text{Seen}} \cap \mathcal{Y}_{\text{Unseen}} = \emptyset$ and $P(\mathcal{D}_s) \neq P(\mathcal{D}_t)$. **3. Single-Source Multi-Target Domain Generalization (DG):** The model, trains on a single source domain

and evaluates on multiple unseen target domains in a closed-set setting, where $\mathcal{Y}_{\text{Seen}} \cap \mathcal{Y}_{\text{Unseen}} = \mathcal{Y}_{\text{Seen}} \cup \mathcal{Y}_{\text{Unseen}}$ but $P(\mathcal{D}_s) \neq P(\mathcal{D}_t)$.

Base-to-New Class Generalization (B2N): Table 1 summarizes the B2N class generalization results across four RS datasets, using the harmonic mean (HM) to balance accuracy between base and new classes. FrogDogNet achieves the best performance, surpassing existing methods on all datasets. Compared to CLIP’s zero-shot approach, it enhances base class accuracy by 35.16% and new class accuracy by 9.30% on average. It also significantly improves upon adaptation-based techniques like CoOp and CoCoOp, with 7.79% and 6.76% higher average HM-scores, respectively. Moreover, FrogDogNet outperforms StyLIP, with a 3.91% boost in the average HM-score, highlighting its superior ability to generalize to unseen classes.

Cross-Dataset Generalization (CD): Table 2 compares CD generalization results, treating target domains as unseen (zero-shot). Using PatternNet as the source, FrogDogNet outperforms all baselines on RSICD, RESISC45, and MLRSNet. Notably, it improves upon CLIP’s zero-shot accuracy by 9.85%, 7.74%, and 7.17%, respectively, and surpasses adaptation-based approaches like CoOp, CoCoOp, and StyLIP. Compared to StyLIP, FrogDogNet achieves gains of 6.98%, 6.41%, and 5.36% on RSICD, RESISC45, and MLRSNet, respectively, demonstrating superior robustness under domain and label shifts.

Single-Source Multi-Target Domain Generalization (DG): Table 3 reports DG results on **v2** datasets, where 16 identical classes span all domains. We use PatternNetv2 as the source and rest all as the targets. FrogDogNet obtains the highest accuracy on RSICDv2 (82.50%), RESISC45v2 (86.90%), and MLRSNetv2 (80.70%). Against StyLIP, it offers improvements of 1.83%, 2.34%, and 5.04% on RSICDv2, RESISC45v2, and MLRSNetv2, respectively, setting a new state of the art in DG. Although StyLIP slightly surpasses FrogDogNet on source by 0.05%, our sizable gains on the targets confirm robust generalization.

4.2. Ablation analysis

Feature space visualization: Figure 4 illustrates a t-SNE [102] plot comparing the image embeddings produced by FFB of FrogDogNet and Meta-Net of CoCoOp [138] on one of the target datasets RSICDv2 for the single-source multi-target domain generalization (DG) task. The results highlight FrogDogNet’s ability to form well-separated clusters for each class, whereas CoCoOp exhibits significant overlap between class clusters. This demonstrates the superior discriminability of FrogDogNet in feature space.

Sensitivity to variation in the number of shots: We assess the performance of FrogDogNet by varying the number of shots from 1 to 32 for the B2N class generalization task and compare it against some of the major SOTA prompting tech-

Method	PatternNet			RSICD			RESISC45			MLRSNet			Avg. of all		
	Base	New	HM	Base	New	HM	Base	New	HM	Base	New	HM	Base	New	HM
CLIP [81]	63.67	64.37	64.02	54.61	55.33	54.97	56.32	55.38	55.85	51.43	51.92	51.67	56.51	56.75	56.63
CoOp [139]	91.62	62.23	74.12	92.52	56.08	69.83	89.04	55.75	68.57	75.21	53.64	62.62	87.10	56.93	68.85
CLIP-Adapter [31]	82.15	63.26	71.48	78.93	55.44	65.13	81.67	56.23	66.60	71.64	53.19	61.05	78.60	57.03	66.10
CoCoOp [138]	92.39	63.34	75.16	93.18	58.67	72.00	89.78	57.18	69.86	76.32	52.75	62.38	87.92	57.99	69.88
ProGrad [140]	92.65	62.48	74.63	93.44	58.15	71.69	90.13	57.89	70.50	75.96	52.23	61.90	88.05	57.69	69.70
MaPLe [45]	94.74	66.12	77.88	94.91	60.52	73.91	91.45	60.82	73.05	79.06	54.85	64.59	90.04	60.57	72.36
APPLeNet [95]	94.89	65.57	77.55	95.26	60.71	74.16	91.24	60.46	72.73	78.53	56.41	65.66	89.98	60.79	72.56
StyLIP [7]	95.13	66.78	78.47	94.98	60.92	74.23	90.87	60.34	72.52	80.65	55.47	65.73	90.41	60.87	72.73
FrogDogNet (ours)	95.50	77.60	85.63	95.70	64.10	76.68	90.60	65.00	75.69	84.90	57.50	68.56	91.67	66.05	76.64
Δ (FrogDogNet - StyLIP)	+0.37	+10.82	+7.16	+0.72	+3.18	+2.45	-0.27	+4.66	+3.17	+4.25	+2.03	+2.83	+1.26	+5.18	+3.91

Table 1. Comparison of FrogDogNet with state-of-the-art methods for the base-to-new (B2N) class generalization task. We present the accuracy for both Base and New classes, with HM denoting the harmonic mean used to evaluate the trade-off between them. The best results are shown in **bold**. Δ shows the performance gap with StyLIP, where green (+) indicates improvement and red (-) indicates a drop.

Method	Source		Target	
	PatternNet	RSICD	RESISC45	MLRSNet
CLIP [81]	61.72	43.25	48.56	45.13
CoOp [139]	85.23	42.53	49.34	44.50
CLIP-Adapter [31]	74.27	42.57	49.07	44.17
CoCoOp [138]	85.95	43.61	49.53	44.72
ProGrad [140]	86.14	41.25	48.26	44.12
MaPLe [45]	87.92	45.23	49.56	46.37
APPLeNet [95]	88.17	44.87	50.97	46.83
StyLIP [7]	88.01	46.12	49.89	46.94
FrogDogNet (ours)	91.60	53.10	56.30	52.30
Δ (FrogDogNet - StyLIP)	+3.59	+6.98	+6.41	+5.36

Table 2. Comparison of FrogDogNet with state-of-the-art methods for cross-dataset (CD) generalization with PatternNet dataset as the source domain and remaining RS datasets as the target domains. We use the accuracy metric as the performance measure. The best results are highlighted in **bold**.

Method	Source		Target	
	PatternNetv2	RSICDv2	RESISC45v2	MLRSNetv2
ERM [105]	73.69	61.40	61.59	61.13
CLIP [81]	78.04	72.15	75.42	67.78
DANN [30]	93.56	75.49	76.18	70.53
CoOp [139]	94.25	76.50	77.87	70.97
CLIP-Adapter [31]	92.36	79.17	79.76	71.04
CoCoOp [138]	94.41	79.33	80.43	71.67
ProGrad [140]	95.18	77.46	80.65	72.29
MaPLe [45]	96.52	80.45	83.37	76.15
APPLeNet [95]	96.63	81.03	82.23	74.03
StyLIP [7]	96.85	80.67	84.56	75.66
FrogDogNet (ours)	96.80	82.50	86.90	80.70
Δ (FrogDogNet - StyLIP)	-0.05	+1.83	+2.34	+5.04

Table 3. Comparing FrogDogNet with state-of-the-art methods for single-source multi-target domain generalization (DG) on **V2** RS datasets. We use the accuracy metric as the performance measure. The best results are highlighted in **bold**.

niques, as presented in Table 4. In this setup, we employ a context length of 4, position the class token at the end, utilize ViT-B/16 as the visual feature backbone, and adopt a unified context vector. We focus on few-shot prompting methods, reporting results on the PatternNet dataset. FrogDogNet consistently surpasses benchmark prompt-learning approaches, achieving at least 11%, 6%, 10.4%, and 0.2% improvements for 4, 8, 16, and 32 shots, respectively.

Sensitivity analysis of FrogDogNet to context lengths: To evaluate the impact of context length on performance of

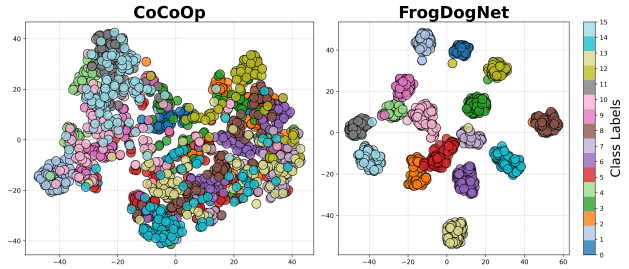


Figure 4. t-SNE plots [103] depicting the image features extracted from the Meta-Net of CoCoOp and the FFB of FrogDogNet for the domain generalization (DG) task on the RSICDv2 dataset. The legends indicate the corresponding class labels.

Method	1-shot	4-shots	8-shots	16-shots	32-shots
CoOp [139]	70.33	71.61	72.17	74.12	74.58
CLIP-Adapter [31]	69.75	69.95	70.37	71.48	71.64
CoCoOp [138]	71.85	73.61	74.53	75.16	74.39
ProGrad [140]	73.67	72.05	73.16	74.63	75.56
APPLeNet [95]	72.44	72.46	75.28	77.55	77.13
FrogDogNet (ours)	73.50	81.70	79.83	85.63	77.28

Table 4. Comparison of FrogDogNet with state-of-the-art methods by varying the number of shots for the B2N class generalization task on the PatternNet dataset. The harmonic mean (HM) of base and new class accuracies is used to evaluate performance and illustrate the generalization trade-off. The best results are in **bold**.

FrogDogNet, we experimented with four different values of \mathcal{M} : 1, 4, 8, and 16 by initializing all \mathcal{M} length prompts in RS. As depicted in Figure 5, FrogDogNet outperforms all major state-of-the-art prompting methods significantly for all context lengths. Notably, FrogDogNet achieves optimal performance at $\mathcal{M} = 4$ among all tested settings.

Effect of RPA loss (\mathcal{L}_{RPA}): Figure 6 presents study on the impact of RPA loss (\mathcal{L}_{RPA}) from Equation 19, comparing FrogDogNet trained with and without \mathcal{L}_{RPA} . Notably, FrogDogNet achieves an average performance gain of 9.3% across all target domain datasets in the CD generalization task with training prompt of "a photo of a" but different testing prompt "satellite photo of a" when \mathcal{L}_{RPA} is incorporated. This highlights the crucial role of \mathcal{L}_{RPA} in enhancing feature alignment, allowing prompt to align better with RS prompt initializations.

¹ We do not consider comparing against [6] and [40] as their reliance on additional self-supervised objectives, contrastive to our model.

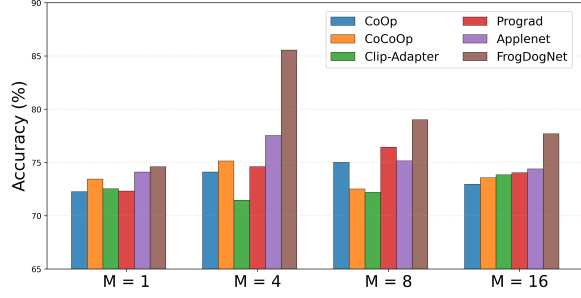


Figure 5. Classification performance of FrogDogNet across context lengths (M) for the B2N generalization task on PatternNet, compared to state-of-the-art methods, using the harmonic mean (HM) of base and new class accuracies.

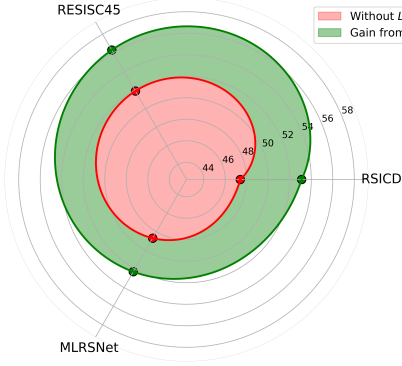


Figure 6. Effect of L_{RPA} on cross-dataset (CD) generalization with PatternNet as the source with prompt "a photo of a" and other RS datasets as the target with prompt "satellite photo of a". We use accuracy as the performance measure.

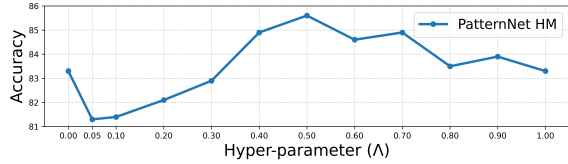


Figure 7. Variation in FrogDogNet's classification performance with different hyper-parameter (Λ) values on the PatternNet dataset for the B2N generalization task, measured using the harmonic mean (HM) of base and new class accuracies.

Insights on hyper-parameter variation: FrogDogNet's performance on the PatternNet dataset fluctuates with different hyper-parameter Λ (in equation 20) values shown in Figure 7. The highest HM score 85.6% occurs at 0.5, while extreme values 0.0 and 1.0 lead to lower performance 83.3%. A stable and strong performance is observed between 0.3 and 0.7, highlighting this range as optimal for balancing base and new class generalization. Similar trends are observed in rest of the datasets (shown in supplementary).

Prompting complexity: Table 5 compares the computational complexity of FrogDogNet on the PatternNet dataset with [138] and [95] for the Base-to-New (B2N) task, measured using [141]. FrogDogNet achieves superior performance (Table 1) while maintaining a complexity of 192.361

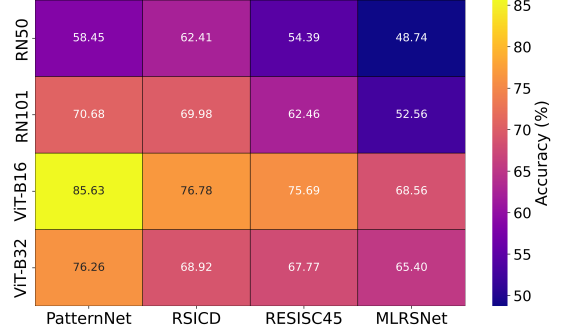


Figure 8. Variation in FrogDogNet's classification performance with different backbone models for the B2N class generalization task across all datasets. The harmonic mean (HM) of base and new class accuracies is used as the evaluation metric.

GFLOPS—15million FLOPS lower than APLeNet and just 0.0047% higher than CoCoOp, highlighting its computational efficiency despite improved performance.

Method	CoCoOp [138]	APLeNet [95]	FrogDogNet (ours)
GFLOPS	192.352	192.376	192.361

Table 5. Comparison of computational complexity of FrogDogNet on the PatternNet dataset in B2N setting, where GFLOPS indicate Giga Floating Point Operations Per Second.

Backbone selection for FrogDogNet: We evaluate FrogDogNet's performance using different backbone models—RN50, RN101, ViT-B16, and ViT-B32—across all four datasets. As shown in Figure 8, ViT-B16 consistently achieves the highest accuracy across all datasets, demonstrating its superior feature representation capabilities.

5. Conclusions

This paper introduces **FrogDogNet**, a prompt learning framework that integrates Fourier frequency filtering to improve domain generalization in remote sensing. To address CLIP's limited generalization on remote sensing images, we introduce a novel approach that combines Fourier-based invariant feature retention with self-attention for more effective prompt learning. FrogDogNet first applies projection and self-attention to refine image features, then removes noise and background artifacts by selectively retaining essential low-frequency components before feeding them into the prompt learning process. This strategy enables better generalization by preserving invariant features within a class, making it more robust across diverse domains.

Extensive experiments demonstrate its superiority over existing prompt learning methods. While frequency-based filtering is widely used in image processing, its application to domain generalization remains underexplored. This work introduces a novel perspective, opening avenues for broader applications across various generalization tasks.

References

- [1] T. Abdullah, Y. Bazi, M. M. Al Rahhal, M. L. Mekhalafi, L. Rangarajan, and M. Zuair. Texts: Deep bidirectional triplet network for matching text to remote sensing images. *Remote Sensing*, 12(3):405, 2020. [3](#)
- [2] Dalal Alajaji, Haikel S. Alhichri, Nassim Ammour, and Naif Alajlan. Few-shot learning for remote sensing scene classification. In *2020 Mediterranean and Middle-East Geoscience and Remote Sensing Symposium (M2GARSS)*, pages 81–84, 2020. [2](#)
- [3] Stanislaw Antol, Aishwarya Agrawal, Jiasen Lu, Margaret Mitchell, Dhruv Batra, C Lawrence Zitnick, and Devi Parikh. Vqa: Visual question answering. In *Proceedings of the IEEE international conference on computer vision*, pages 2425–2433, 2015. [3](#)
- [4] Yogesh Balaji, Swami Sankaranarayanan, and Rama Chellappa. Metareg: Towards domain generalization using meta-regularization. *Advances in neural information processing systems*, 31, 2018. [2](#)
- [5] Y. Bazi, M. M. A. Rahhal, M. L. Mekhalafi, M. A. Al Zuair, and F. Melgani. Bi-modal transformer-based approach for visual question answering in remote sensing imagery. *IEEE Transactions on Geoscience and Remote Sensing*, 60:1–11, 2022. [3](#)
- [6] Avigyan Bhattacharya, Mainak Singha, Ankit Jha, and Biplob Banerjee. C-saw: Self-supervised prompt learning for image generalization in remote sensing. In *Proceedings of the Fourteenth Indian Conference on Computer Vision, Graphics and Image Processing*, pages 1–10, 2023. [2](#), [3](#), [7](#)
- [7] Shirsha Bose, Ankit Jha, Enrico Fini, Mainak Singha, Elisa Ricci, and Biplob Banerjee. Stylip: Multi-scale style-conditioned prompt learning for clip-based domain generalization. *arXiv preprint arXiv:2302.09251*, 2024. Accepted in WACV 2024. [2](#), [3](#), [7](#)
- [8] Qinglong Cao, Zhengqin Xu, Yuntian Chen, Chao Ma, and Xiaokang Yang. Domain-controlled prompt learning. In *Proceedings of the AAAI Conference on Artificial Intelligence*, pages 936–944, 2024. [3](#)
- [9] Qinglong Cao, Zhengqin Xu, Yuntian Chen, Chao Ma, and Xiaokang Yang. Domain prompt learning with quaternion networks. In *Proceedings of the IEEE/CVF Conference on Computer Vision and Pattern Recognition*, pages 26637–26646, 2024. [3](#)
- [10] C. Chappuis, V. Mendez, E. Walt, S. Lobry, B. Le Saux, and D. Tuia. Language transformers for remote sensing visual question answering. In *IGARSS 2022-2022 IEEE International Geoscience and Remote Sensing Symposium*, pages 4855–4858. IEEE, 2022. [3](#)
- [11] Prithvijit Chattopadhyay, Yogesh Balaji, and Judy Hoffman. Learning to balance specificity and invariance for in and out of domain generalization. In *European Conference on Computer Vision*, pages 301–318. Springer, 2020. [2](#)
- [12] Keyan Chen, Chenyang Liu, Hao Chen, Haotian Zhang, Wenyan Li, Zhengxia Zou, and Zhenwei Shi. Rsprompter: Learning to prompt for remote sensing instance segmentation based on visual foundation model. *IEEE Transactions on Geoscience and Remote Sensing*, 2024. [3](#)
- [13] Mingyang Chen, Wen Zhang, Wei Zhang, Qiang Chen, and Huajun Chen. Meta relational learning for few-shot link prediction in knowledge graphs. *arXiv preprint arXiv:1909.01515*, 2019. [2](#)
- [14] Y. Chen, C. Wei, D. Wang, C. Ji, and B. Li. Semi-supervised contrastive learning for few-shot segmentation of remote sensing images. *Remote Sensing*, 14(17):4254, 2022. [3](#)
- [15] Gong Cheng, Junwei Han, and Xiaoqiang Lu. Remote sensing image scene classification: Benchmark and state of the art. *Proceedings of the IEEE*, 105(10):1865–1883, 2017. [6](#)
- [16] Q. Cheng, Y. Zhou, P. Fu, Y. Xu, and L. Zhang. A deep semantic alignment network for the cross-modal image-text retrieval in remote sensing. *IEEE Journal of Selected Topics in Applied Earth Observations and Remote Sensing*, 14: 4284–4297, 2021. [3](#)
- [17] J. W. Cooley and J. W. Tukey. An algorithm for the machine calculation of complex fourier series. *Mathematics of Computation*, 19(90):297–301, 1965. [4](#)
- [18] MRSB DATA. Multimodal artificial intelligence foundation models: Unleashing the power of remote sensing big data in earth observation. *Innovation*, 2(1):100055, 2024. [1](#)
- [19] Jacob Devlin, Ming-Wei Chang, Kenton Lee, and Kristina Toutanova. Bert: Pre-training of deep bidirectional transformers for language understanding. *arXiv preprint arXiv:1810.04805*, 2018. [3](#)
- [20] Jacob Devlin, Ming-Wei Chang, Kenton Lee, and Kristina Toutanova. Bert: Pre-training of deep bidirectional transformers for language understanding. *arXiv preprint arXiv:1810.04805*, 2018. [3](#)
- [21] S. Dong, L. Wang, B. Du, and X. Meng. Changeclip: Remote sensing change detection with multimodal vision-language representation learning. *ISPRS Journal of Photogrammetry and Remote Sensing*, 208:53–69, 2024. [2](#)
- [22] Alexey Dosovitskiy. An image is worth 16x16 words: Transformers for image recognition at scale. *arXiv preprint arXiv:2010.11929*, 2020. [3](#)
- [23] Alexey Dosovitskiy, Lucas Beyer, Alexander Kolesnikov, Dirk Weissenborn, Xiaohua Zhai, Thomas Unterthiner, Mostafa Dehghani, Matthias Minderer, Georg Heigold, Sylvain Gelly, Jakob Uszkoreit, and Neil Houlsby. An image is worth 16x16 words: Transformers for image recognition at scale. *CoRR*, abs/2010.11929, 2020. [3](#)
- [24] Qi Dou, Daniel Coelho de Castro, Konstantinos Kamnitsas, and Ben Glocker. Domain generalization via model-agnostic learning of semantic features. *Advances in Neural Information Processing Systems*, 32, 2019. [2](#)
- [25] Efkani Duraklı and Erchan Aptoula. Domain generalized object detection for remote sensing images. In *2023 31st Signal Processing and Communications Applications Conference (SIU)*, pages 1–4, 2023. [1](#)
- [26] Abolfazl Farahani, Sahar Voghoei, Khaled Rasheed, and Hamid R Arabnia. A brief review of domain adaptation. *Advances in data science and information engineering*, pages 877–894, 2021. [1](#)
- [27] Chelsea Finn, Pieter Abbeel, and Sergey Levine. Model-agnostic meta-learning for fast adaptation of deep networks.

- In *International conference on machine learning*, pages 1126–1135. PMLR, 2017. 2
- [28] Chelsea Finn, Pieter Abbeel, and Sergey Levine. Model-agnostic meta-learning for fast adaptation of deep networks. In *International conference on machine learning*, pages 1126–1135. PMLR, 2017. 2
- [29] Yaroslav Ganin and Victor Lempitsky. Unsupervised domain adaptation by backpropagation. In *International Conference on Machine Learning*, pages 1180–1189. PMLR, 2015. 1
- [30] Yaroslav Ganin, Evgeniya Ustinova, Hana Ajakan, Pascal Germain, Hugo Larochelle, François Laviolette, Mario Marchand, and Victor Lempitsky. Domain-adversarial training of neural networks. *The journal of machine learning research*, 17(1):2096–2030, 2016. 7
- [31] Peng Gao, Shijie Geng, Renrui Zhang, Teli Ma, Rongyao Fang, Yongfeng Zhang, Hongsheng Li, and Yu Qiao. Clip-adapter: Better vision-language models with feature adapters. *arXiv preprint arXiv:2110.04544*, 2021. 2, 3, 7
- [32] Ali Ghanbarzadeh and Hossein Soleimani. Self-supervised in-domain representation learning for remote sensing image scene classification. *Heliyon*, 10(19):e37962, 2024. 1
- [33] Changsheng Xu Hantao Yao, Rui Zhang. Visual-language prompt tuning with knowledge-guided context optimization. In *The IEEE/CVF Conference on Computer Vision and Pattern Recognition*, 2023. 5
- [34] Kaiming He, Xiangyu Zhang, Shaoqing Ren, and Jian Sun. Deep residual learning for image recognition. In *Proceedings of the IEEE conference on computer vision and pattern recognition*, pages 770–778, 2016. 3
- [35] Miyuki Hino, Elinor Benami, and Nina Brooks. Machine learning for environmental monitoring. *Nature Sustainability*, 1(10):583–588, 2018. 1
- [36] Yijiang Hu and Hong Tang. On the generalization ability of a global model for rapid building mapping from heterogeneous satellite images of multiple natural disaster scenarios. *Remote Sensing*, 13(5):984, 2021. 1
- [37] Y. Hu, J. Yuan, C. Wen, X. Lu, and X. Li. Rsgpt: A remote sensing vision language model and benchmark. *arXiv preprint arXiv:2307.15266*, 2023. 3
- [38] Zeyi Huang, Haohan Wang, Eric P Xing, and Dong Huang. Self-challenging improves cross-domain generalization. In *European Conference on Computer Vision*, pages 124–140. Springer, 2020. 2
- [39] Jordi Inglada and Alain Giros. On the real capabilities of remote sensing for disaster management-feedback from real cases. In *IGARSS 2004. 2004 IEEE International Geoscience and Remote Sensing Symposium*, pages 1110–1112. IEEE, 2004. 1
- [40] Ankit Jha, Mainak Singha, Avigyan Bhattacharya, and Biplob Banerjee. Rs3lip: Consistency for remote sensing image classification on part embeddings using self-supervised learning and clip. *Computer Vision and Image Understanding*, 251:104254, 2025. 3, 7
- [41] Hong Ji, Zhi Gao, Yongjun Zhang, Yu Wan, Can Li, and Tiancan Mei. Few-shot scene classification of optical remote sensing images leveraging calibrated pretext tasks. *IEEE Transactions on Geoscience and Remote Sensing*, 60: 1–13, 2022. 2
- [42] Chao Jia, Yinfei Yang, Ye Xia, Yi-Ting Chen, Zarana Parekh, Hieu Pham, Quoc Le, Yun-Hsuan Sung, Zhen Li, and Tom Duerig. Scaling up visual and vision-language representation learning with noisy text supervision. In *International Conference on Machine Learning*, pages 4904–4916. PMLR, 2021. 2
- [43] Chao Jia, Yinfei Yang, Ye Xia, Yi-Ting Chen, Zarana Parekh, Hieu Pham, Quoc Le, Yun-Hsuan Sung, Zhen Li, and Tom Duerig. Scaling up visual and vision-language representation learning with noisy text supervision. In *Proceedings of the 38th International Conference on Machine Learning*, pages 4904–4916. PMLR, 2021. 2
- [44] X. Jiang, N. Zhou, and X. Li. Few-shot segmentation of remote sensing images using deep metric learning. *IEEE Geoscience and Remote Sensing Letters*, 19:1–5, 2022. 3
- [45] Muhammad Uzair Khattak, Hanoona Rasheed, Muhammad Maaz, Salman Khan, and Fahad Shahbaz Khan. Maple: Multi-modal prompt learning. *arXiv preprint arXiv:2210.03117*, 2023. Accepted at CVPR 2023. 2, 3, 7
- [46] Long Lan, Fengxiang Wang, Xiangtao Zheng, Zengmao Wang, and Xinwang Liu. Efficient prompt tuning of large vision-language model for fine-grained ship classification. *IEEE Transactions on Geoscience and Remote Sensing*, 2024. 3
- [47] A. Li, Z. Lu, L. Wang, T. Xiang, and J.-R. Wen. Zero-shot scene classification for high spatial resolution remote sensing images. *IEEE Transactions on Geoscience and Remote Sensing*, 55(7):4157–4167, 2017. 3
- [48] Da Li, Yongxin Yang, Yi-Zhe Song, and Timothy Hospedales. Learning to generalize: Meta-learning for domain generalization. In *Proceedings of the AAAI conference on artificial intelligence*, 2018. 1, 2
- [49] Da Li, Jianshu Zhang, Yongxin Yang, Cong Liu, Yi-Zhe Song, and Timothy M Hospedales. Episodic training for domain generalization. In *Proceedings of the IEEE/CVF International Conference on Computer Vision*, pages 1446–1455, 2019. 2
- [50] Hongzhi Li, Joseph G Ellis, Lei Zhang, and Shih-Fu Chang. Patternnet: Visual pattern mining with deep neural network. In *Proceedings of the 2018 ACM on international conference on multimedia retrieval*, pages 291–299, 2018. 6
- [51] Haoliang Li, Sinno Jialin Pan, Shiqi Wang, and Alex C Kot. Domain generalization with adversarial feature learning. In *Proceedings of the IEEE conference on computer vision and pattern recognition*, pages 5400–5409, 2018. 2
- [52] Junnan Li, Dong Li, Silvio Savarese, and Steven C. Hoi. Blip-2: Bootstrapping language-image pre-training with frozen image encoders and large language models. In *International conference on machine learning*, pages 19730–19742. PMLR, 2023. 3
- [53] Lei Li, Ke Gao, Juan Cao, Ziyao Huang, Yepeng Weng, Xiaoyue Mi, Zhengze Yu, Xiaoya Li, and Boyang Xia. Progressive domain expansion network for single domain generalization. In *Proceedings of the IEEE/CVF Conference on*

Computer Vision and Pattern Recognition, pages 224–233, 2021. 2

- [54] Liunian Harold Li, Mark Yatskar, Da Yin, Cho-Jui Hsieh, and Kai-Wei Chang. Visualbert: A simple and performant baseline for vision and language. *arXiv preprint arXiv:1908.03557*, 2019. 2
- [55] X. Li, X. Zhang, W. Huang, and Q. Wang. Truncation cross entropy loss for remote sensing image captioning. *IEEE Transactions on Geoscience and Remote Sensing*, 59(6): 5246–5257, 2020. 3
- [56] Xiang Li, Congcong Wen, Yuan Hu, and Nan Zhou. RS-CLIP: Zero-Shot Remote Sensing Scene Classification via Contrastive Vision-Language Supervision. *International Journal of Applied Earth Observation and Geoinformation*, 124:103497, 2023. 2
- [57] Xiang Li, Congcong Wen, Yuan Hu, Zhenghang Yuan, and Xiao Xiang Zhu. Vision-language models in remote sensing: Current progress and future trends. *IEEE Geoscience and Remote Sensing Magazine*, 2024. 3
- [58] Ya Li, Xinmei Tian, Mingming Gong, Yajing Liu, Tongliang Liu, Kun Zhang, and Dacheng Tao. Deep domain generalization via conditional invariant adversarial networks. In *Proceedings of the European conference on computer vision (ECCV)*, pages 624–639, 2018. 2
- [59] Yiyang Li, Yongxin Yang, Wei Zhou, and Timothy Hospedales. Feature-critic networks for heterogeneous domain generalization. In *International Conference on Machine Learning*, pages 3915–3924. PMLR, 2019. 2
- [60] Y. Li, S. Fang, L. Jiao, R. Liu, and R. Shang. A multi-level attention model for remote sensing image captions. *Remote Sensing*, 12(6):939, 2020. 3
- [61] Z. Li, D. Zhang, Y. Wang, D. Lin, and J. Zhang. Generative adversarial networks for zero-shot remote sensing scene classification. *Applied Sciences*, 12(8):3760, 2022. 3
- [62] Ziming Li, Bin Chen, Shengbiao Wu, Mo Su, Jing M. Chen, and Bing Xu. Deep learning for urban land use category classification: A review and experimental assessment. *Remote Sensing of Environment*, 311:114290, 2024. 1
- [63] Hui Lin, Chao Zhang, Danfeng Hong, Kexin Dong, and Congcong Wen. Fedrscip: Federated learning for remote sensing scene classification using vision-language models. *arXiv preprint arXiv:2501.02461*, 2025. 3
- [64] Bing Liu, Xuchu Yu, Anzhu Yu, Pengqiang Zhang, Gang Wan, and Ruirui Wang. Deep few-shot learning for hyperspectral image classification. *IEEE Transactions on Geoscience and Remote Sensing*, 57(4):2290–2304, 2018. 2
- [65] Fan Liu, Delong Chen, Zhangqingyun Guan, Xiaocong Zhou, Jiale Zhu, Qiaolin Ye, Liyong Fu, and Jun Zhou. RemoteCLIP: A Vision-Language Foundation Model for Remote Sensing. *IEEE Transactions on Geoscience and Remote Sensing*, 62:5622216, 2024. 2
- [66] S. Lobry, D. Marcos, J. Murray, and D. Tuia. Rsvqa: Visual question answering for remote sensing data. *IEEE Transactions on Geoscience and Remote Sensing*, 58(12):8555–8566, 2020. 3
- [67] Xiaoqiang Lu, Binqiang Wang, Xiangtao Zheng, and Xuelong Li. Exploring models and data for remote sensing image caption generation. *IEEE Transactions on Geoscience and Remote Sensing*, 56(4):2183–2195, 2017. 3, 6
- [68] X. Lu, X. Sun, W. Diao, Y. Mao, J. Li, Y. Zhang, P. Wang, and K. Fu. Few-shot object detection in aerial imagery guided by text-modal knowledge. *IEEE Transactions on Geoscience and Remote Sensing*, 2023. 3
- [69] Lei Ma, Yu Liu, Xueliang Zhang, Yuanxin Ye, Gaoferi Yin, and Brian Alan Johnson. Deep learning in remote sensing applications: A meta-analysis and review. *ISPRS Journal of Photogrammetry and Remote Sensing*, 152:166–177, 2019. 1
- [70] M. Martini, V. Mazzia, A. Khaliq, and M. Chiaberge. Domain-adversarial training of self-attention-based networks for land cover classification using multi-temporal sentinel-2 satellite imagery. *Remote Sensing*, 13(13):2564, 2021. 1
- [71] Toshihiko Matsuura and Tatsuya Harada. Domain generalization using a mixture of multiple latent domains. In *Proceedings of the AAAI conference on artificial intelligence*, pages 11749–11756, 2020. 2
- [72] Peter J Morley, Daniel NM Donoghue, Jan-Chang Chen, and Alistair S Jump. Integrating remote sensing and demography for more efficient and effective assessment of changing mountain forest distribution. *Ecological Informatics*, 43:106–115, 2018. 1
- [73] Debabrata Pal, Valay Bunde, Biplab Banerjee, and Yogananda Jeppu. Spn: Stable prototypical network for few-shot learning-based hyperspectral image classification. *IEEE Geoscience and Remote Sensing Letters*, 19:1–5, 2021. 2
- [74] Claudio Persello and Lorenzo Bruzzone. Relevant and invariant feature selection of hyperspectral images for domain generalization. In *2014 IEEE Geoscience and Remote Sensing Symposium*, pages 3562–3565. IEEE, 2014. 2
- [75] Fabio Petroni, Tim Rocktäschel, Patrick Lewis, Anton Bakhtin, Yuxiang Wu, Alexander H Miller, and Sebastian Riedel. Language models as knowledge bases? *arXiv preprint arXiv:1909.01066*, 2019. 3
- [76] Xiaoman Qi, Panpan Zhu, Yuebin Wang, Liqiang Zhang, Junhuan Peng, Mengfan Wu, Jialong Chen, Xudong Zhao, Ning Zang, and P Takis Mathiopoulos. Mlrsnet: A multi-label high spatial resolution remote sensing dataset for semantic scene understanding. *ISPRS Journal of Photogrammetry and Remote Sensing*, 169:337–350, 2020. 6
- [77] Fengchun Qiao and Xi Peng. Uncertainty-guided model generalization to unseen domains. In *Proceedings of the IEEE/CVF conference on computer vision and pattern recognition*, pages 6790–6800, 2021. 2
- [78] Fengchun Qiao, Long Zhao, and Xi Peng. Learning to learn single domain generalization. In *Proceedings of the IEEE/CVF Conference on Computer Vision and Pattern Recognition*, pages 12556–12565, 2020. 2
- [79] J. Quan, C. Wu, H. Wang, and Z. Wang. Structural alignment based zero-shot classification for remote sensing scenes. In *2018 IEEE International Conference on Electronics and Communication Engineering (ICECE)*, pages 17–21. IEEE, 2018. 3

- [80] Alec Radford. Improving language understanding by generative pre-training. 2018. [3](#)
- [81] Alec Radford, Jong Wook Kim, Chris Hallacy, Aditya Ramesh, Gabriel Goh, Sandhini Agarwal, Girish Sastry, Amanda Askell, Pamela Mishkin, Jack Clark, et al. Learning transferable visual models from natural language supervision. In *International Conference on Machine Learning*, pages 8748–8763. PMLR, 2021. [2](#), [3](#), [7](#)
- [82] Alec Radford, Jong Wook Kim, Chris Hallacy, Aditya Ramesh, Gabriel Goh, Sandhini Agarwal, Girish Sastry, Amanda Askell, Pamela Mishkin, Jack Clark, et al. Learning transferable visual models from natural language supervision. In *International Conference on Machine Learning*, pages 8748–8763. PMLR, 2021. [2](#)
- [83] M. M. A. Rahhal, Y. Bazi, T. Abdullah, M. L. Mekhalfi, and M. Zuair. Deep unsupervised embedding for remote sensing image retrieval using textual cues. *Applied Sciences*, 10(24):8931, 2020. [3](#)
- [84] M. M. A. Rahhal, Y. Bazi, S. O. Alsaleh, M. Al-Razgan, M. L. Mekhalfi, M. Al Zuair, and N. Alajlan. Open-ended remote sensing visual question answering with transformers. *International Journal of Remote Sensing*, 43(18):6809–6823, 2022. [3](#)
- [85] M. M. A. Rahhal, Y. Bazi, N. A. Alsharif, L. Bashmal, N. Alajlan, and F. Melgani. Multilanguage transformer for improved text to remote sensing image retrieval. *IEEE Journal of Selected Topics in Applied Earth Observations and Remote Sensing*, 15:9115–9126, 2022. [3](#)
- [86] M. M. A. Rahhal, M. A. Bencherif, Y. Bazi, A. Alharbi, and M. L. Mekhalfi. Contrasting dual transformer architectures for multi-modal remote sensing image retrieval. *Applied Sciences*, 13(1):282, 2023. [3](#)
- [87] Yuyu Rao, Wenliang Zhao, Zhen Zhu, Jiwen Lu, and Jie Zhou. Global filter networks for image classification. In *Proceedings of the Advances in Neural Information Processing Systems (NeurIPS)*, pages 980–993, 2021. [4](#)
- [88] Herbert Robbins and Sutton Monro. A stochastic approximation method. *The annals of mathematical statistics*, pages 400–407, 1951. [6](#)
- [89] Marc Russwurm, Sherrie Wang, Marco Korner, and David Lobell. Meta-learning for few-shot land cover classification. In *Proceedings of the IEEE/CVF Conference on Computer Vision and Pattern Recognition (CVPR) Workshops*, 2020. [2](#)
- [90] Floyd F. Sabins. Remote sensing for mineral exploration. *Ore Geology Reviews*, 14(3-4):157–183, 1999. [1](#)
- [91] Sudipan Saha, Shan Zhao, and Xiao Xiang Zhu. Multi-target domain adaptation for remote sensing classification using graph neural network. *IEEE Geoscience and Remote Sensing Letters*, 19:1–5, 2022. [1](#)
- [92] Z. Shi and Z. Zou. Can a machine generate humanlike language descriptions for a remote sensing image? *IEEE Transactions on Geoscience and Remote Sensing*, 55(6):3623–3634, 2017. [3](#)
- [93] Taylor Shin, Yasaman Razeghi, Robert L Logan IV, Eric Wallace, and Sameer Singh. Autoprompt: Eliciting knowledge from language models with automatically generated prompts. *arXiv preprint arXiv:2010.15980*, 2020. [3](#)
- [94] Manli Shu, Weili Nie, De-An Huang, Zhiding Yu, Tom Goldstein, Anima Anandkumar, and Chaowei Xiao. Test-time prompt tuning for zero-shot generalization in vision-language models. *arXiv preprint arXiv:2209.07511*, 2022. [3](#)
- [95] Mainak Singha, Ankit Jha, Bhupendra Solanki, Shirsha Bose, and Biplab Banerjee. Applenet: Visual attention parameterized prompt learning for few-shot remote sensing image generalization using clip. In *Proceedings of the IEEE/CVF Conference on Computer Vision and Pattern Recognition*, 2023. [2](#), [3](#), [6](#), [7](#), [8](#)
- [96] Kihyuk Sohn. Improved deep metric learning with multi-class n-pair loss objective. In *Advances in Neural Information Processing Systems*, 2016. [3](#)
- [97] G. Sumbul, R. G. Cinbis, and S. Aksoy. Fine-grained object recognition and zero-shot learning in remote sensing imagery. *IEEE Transactions on Geoscience and Remote Sensing*, 56(2):770–779, 2017. [3](#)
- [98] C Szegedy. Intriguing properties of neural networks. *arXiv preprint arXiv:1312.6199*, 2013. [2](#)
- [99] Naftali Tishby, Fernando C Pereira, and William Bialek. The information bottleneck method. *arXiv preprint physics/0004057*, 2000. [2](#)
- [100] Devis Tuia, Claudio Persello, and Lorenzo Bruzzone. Domain adaptation for the classification of remote sensing data: An overview of recent advances. *IEEE Geoscience and Remote Sensing Magazine*, 4(2):41–57, 2016. [1](#)
- [101] Devis Tuia, Ribana Roscher, Jan Dirk Wegner, Narun Jacobs, Xiao Xiang Zhu, and Gustau Camps-Valls. Toward a collective agenda on ai for earth science data analysis. *IEEE Geoscience and Remote Sensing Magazine*, 9(2):88–104, 2021. [3](#)
- [102] Laurens Van der Maaten and Geoffrey Hinton. Visualizing data using t-sne. *Journal of machine learning research*, 9(11), 2008. [6](#)
- [103] Laurens Van der Maaten and Geoffrey Hinton. Visualizing data using t-sne. *Journal of machine learning research*, 9(11), 2008. [7](#)
- [104] CJ Van Westen. Remote sensing for natural disaster management. *International archives of photogrammetry and remote sensing*, 33(B7/4; PART 7):1609–1617, 2000. [1](#)
- [105] Vladimir N. Vapnik. *Statistical Learning Theory*. Wiley-Interscience, 1998. [7](#)
- [106] Ashish Vaswani, Noam Shazeer, Niki Parmar, Jakob Uszkoreit, Llion Jones, Aidan N Gomez, Łukasz Kaiser, and Ilya Polosukhin. Attention is all you need. In *Advances in neural information processing systems*, pages 5998–6008, 2017. [2](#)
- [107] Oriol Vinyals, Alexander Toshev, Samy Bengio, and Dumitru Erhan. Show and tell: A neural image caption generator. In *Proceedings of the IEEE conference on computer vision and pattern recognition*, pages 3156–3164, 2015. [3](#)
- [108] Riccardo Volpi, Hongseok Namkoong, Ozan Sener, John C Duchi, Vittorio Murino, and Silvio Savarese. Generalizing to unseen domains via adversarial data augmentation. *Advances in neural information processing systems*, 31, 2018. [2](#)

- [109] C. Wang, G. Peng, and B. De Baets. A distance-constrained semantic autoencoder for zero-shot remote sensing scene classification. *IEEE Journal of Selected Topics in Applied Earth Observations and Remote Sensing*, 14:12545–12556, 2021. [3](#)
- [110] Libo Wang, Sijun Dong, Ying Chen, Xiaoliang Meng, Shenghui Fang, and Songlin Fei. Metasegnet: Metadata-collaborative vision-language representation learning for semantic segmentation of remote sensing images. *IEEE Transactions on Geoscience and Remote Sensing*, 2024. [3](#)
- [111] Q. Wang, W. Huang, X. Zhang, and X. Li. Word-sentence framework for remote sensing image captioning. *IEEE Transactions on Geoscience and Remote Sensing*, 59(12):10532–10543, 2020. [3](#)
- [112] Zijian Wang, Yadan Luo, Ruihong Qiu, Zi Huang, and Mahsa Baktashmotlagh. Learning to diversify for single domain generalization. In *Proceedings of the IEEE/CVF International Conference on Computer Vision*, pages 834–843, 2021. [2](#)
- [113] Qinwei Xu, Ruipeng Zhang, Ya Zhang, Yanfeng Wang, and Qi Tian. A fourier-based framework for domain generalization. In *Proceedings of the IEEE/CVF Conference on Computer Vision and Pattern Recognition*, pages 14383–14392, 2021. [2](#)
- [114] Qinwei Xu, Ruipeng Zhang, Yi-Yan Wu, Ya Zhang, Ning Liu, and Yanfeng Wang. Simde: A simple domain expansion approach for single-source domain generalization. In *Proceedings of the IEEE/CVF Conference on Computer Vision and Pattern Recognition*, pages 4798–4808, 2023. [2](#)
- [115] Zhaohui Xue, Yiyang Zhou, and Peijun Du. S3net: Spectral-spatial siamese network for few-shot hyperspectral image classification. *IEEE Transactions on Geoscience and Remote Sensing*, 60:1–19, 2022. [2](#)
- [116] Xi Yang, Dechen Kong, Dong Yang, and Miao Wang. Domain-aware generalized meta-learning for space target recognition. *IEEE Transactions on Geoscience and Remote Sensing*, 62:1–12, 2024. [1](#)
- [117] Xiong Yaoting. Sar-optical image matching model based on contrastive learning. In *2023 20th International Computer Conference on Wavelet Active Media Technology and Information Processing (ICCWAMTIP)*, pages 1–5, 2023. [1](#)
- [118] Lu Yuan, Dongdong Chen, Yi-Ling Chen, Noel Codella, Xiyang Dai, Jianfeng Gao, Houdong Hu, Xuedong Huang, Boxin Li, Chunyuan Li, et al. Florence: A new foundation model for computer vision. *arXiv preprint arXiv:2111.11432*, 2021. [2](#)
- [119] Z. Yuan, W. Zhang, X. Rong, X. Li, J. Chen, H. Wang, K. Fu, and X. Sun. A lightweight multi-scale crossmodal text-image retrieval method in remote sensing. *IEEE Transactions on Geoscience and Remote Sensing*, 60:1–19, 2021. [3](#)
- [120] Z. Yuan, L. Mou, Q. Wang, and X. X. Zhu. From easy to hard: Learning language-guided curriculum for visual question answering on remote sensing data. *IEEE Transactions on Geoscience and Remote Sensing*, 60:1–11, 2022. [3](#)
- [121] Z. Yuan, W. Zhang, K. Fu, X. Li, C. Deng, H. Wang, and X. Sun. Exploring a fine-grained multiscale method for cross-modal remote sensing image retrieval. *IEEE Transactions on Geoscience and Remote Sensing*, 60:3078451, 2022. [3](#)
- [122] Z. Yuan, W. Zhang, C. Tian, X. Rong, Z. Zhang, H. Wang, K. Fu, and X. Sun. Remote sensing cross-modal text-image retrieval based on global and local information. *IEEE Transactions on Geoscience and Remote Sensing*, 60:1–16, 2022. [3](#)
- [123] Xiaohua Zhai, Xiao Wang, Basil Mustafa, Andreas Steiner, Daniel Keysers, Alexander Kolesnikov, and Lucas Beyer. Lit: Zero-shot transfer with locked-image text tuning. In *Proceedings of the IEEE/CVF Conference on Computer Vision and Pattern Recognition*, pages 18123–18133, 2022. [2](#)
- [124] Pei Zhang, Yunpeng Bai, Dong Wang, Bendu Bai, and Ying Li. Few-shot classification of aerial scene images via meta-learning. *Remote Sensing*, 13(1):108, 2021. [2](#)
- [125] S. Zhang, F. Song, X. Liu, X. Hao, Y. Liu, T. Lei, and P. Jiang. Text semantic fusion relation graph reasoning for few-shot object detection on remote sensing images. *Remote Sensing*, 15(5):1187, 2023. [3](#)
- [126] Shijie Zhang, Bin Zhang, Yuntao Wu, Huabing Zhou, Junjun Jiang, and Jiayi Ma. Segclip: Multimodal visual-language and prompt learning for high-resolution remote sensing semantic segmentation. *IEEE Transactions on Geoscience and Remote Sensing*, 2024. [3](#)
- [127] X. Zhang, X. Li, J. An, L. Gao, B. Hou, and C. Li. Natural language description of remote sensing images based on deep learning. In *2017 IEEE International Geoscience and Remote Sensing Symposium (IGARSS)*, pages 4798–4801. IEEE, 2017. [3](#)
- [128] X. Zhang, X. Wang, X. Tang, H. Zhou, and C. Li. Description generation for remote sensing images using attribute attention mechanism. *Remote Sensing*, 11(6):612, 2019. [3](#)
- [129] Y. Zhang, M. Zhang, W. Li, S. Wang, and R. Tao. Language-aware domain generalization network for cross-scene hyperspectral image classification. *IEEE Transactions on Geoscience and Remote Sensing*, 2023. [3](#)
- [130] Z. Zhang, T. Zhao, Y. Guo, and J. Yin. Rs5m: A large scale vision-language dataset for remote sensing vision-language foundation model. *arXiv preprint arXiv:2306.11300*, 2023. [3](#)
- [131] Long Zhao, Ting Liu, Xi Peng, and Dimitris Metaxas. Maximum-entropy adversarial data augmentation for improved generalization and robustness. *Advances in Neural Information Processing Systems*, 33:14435–14447, 2020. [2](#)
- [132] R. Zhao, Z. Shi, and Z. Zou. High-resolution remote sensing image captioning based on structured attention. *IEEE Transactions on Geoscience and Remote Sensing*, 60:1–14, 2021. [3](#)
- [133] Juepeng Zheng, Wenzhao Wu, Shuai Yuan, Haohuan Fu, Weijia Li, and Le Yu. Multisource-domain generalization-based oil palm tree detection using very-high-resolution (vhr) satellite images. *IEEE Geoscience and Remote Sensing Letters*, 19:1–5, 2021. [1](#), [2](#)
- [134] X. Zheng, B. Wang, X. Du, and X. Lu. Mutual attention inception network for remote sensing visual question answering. *IEEE Transactions on Geoscience and Remote Sensing*, 60:1–14, 2021. [3](#)

- [135] Kaiyang Zhou, Yongxin Yang, Timothy Hospedales, and Tao Xiang. Deep domain-adversarial image generation for domain generalisation. In *Proceedings of the AAAI Conference on Artificial Intelligence*, pages 13025–13032, 2020. [2](#)
- [136] Kaiyang Zhou, Yongxin Yang, Yu Qiao, and Tao Xiang. Domain generalization with mixstyle. *arXiv preprint arXiv:2104.02008*, 2021. [2](#)
- [137] Kaiyang Zhou, Ziwei Liu, Yu Qiao, Tao Xiang, and Chen Change Loy. Domain generalization: A survey. *IEEE Transactions on Pattern Analysis and Machine Intelligence*, 2022. [1](#)
- [138] Kaiyang Zhou, Jingkang Yang, Chen Change Loy, and Ziwei Liu. Conditional prompt learning for vision-language models. In *Proceedings of the IEEE/CVF Conference on Computer Vision and Pattern Recognition*, pages 16816–16825, 2022. [2](#), [3](#), [5](#), [6](#), [7](#), [8](#)
- [139] Kaiyang Zhou, Jingkang Yang, Chen Change Loy, and Ziwei Liu. Learning to prompt for vision-language models. *International Journal of Computer Vision*, 130(9):2337–2348, 2022. [2](#), [3](#), [6](#), [7](#)
- [140] Beier Zhu, Yulei Niu, Yucheng Han, Yue Wu, and Hanwang Zhang. Prompt-aligned gradient for prompt tuning. *arXiv preprint arXiv:2205.14865*, 2022. [2](#), [3](#), [7](#)
- [141] Ligeng Zhu. pytorch-opcounter, 2018. Maintained by Lyken17. Available at: pytorch-OpCounter. [8](#)
- [142] Xiao Xiang Zhu, David Tuia, and Lorenzo Mou et al. Deep learning in remote sensing: A comprehensive review and list of resources. *IEEE Geoscience and Remote Sensing Magazine*, 5(4):8–36, 2017. [1](#)
- [143] U. Zia, M. M. Riaz, and A. Ghafoor. Transforming remote sensing images to textual descriptions. *International Journal of Applied Earth Observation and Geoinformation*, 108:102741, 2022. [3](#)